Investigation of Bi_2S_3 nanorods photocatalytic activity under visible light for the degradation of dye from aquatic system

Subramaniyan Keerthana
Alagappa University
Rathinam Yuvakkumar
Alagappa University
Ponnusamy Senthil Kumar (senthilkumarp@ssn.edu.in)
Sri Sivasubramaniya Nadar College of Engineering
Ganesan Ravi
Alagappa University
Dhayalan Velauthapillai
Western Norway University of Applied Sciences - Stord Campus: Hogskulen pa Vestlandet - Campus Stord
Dai-Viet Nguyen Vo
Nguyen Tat Thanh University

Research Article

Keywords: Bi2S3, solvothermal, Ethylene glycol, bandgap, nanorods, Methylene blue, visible light

Posted Date: April 13th, 2021

DOI: https://doi.org/10.21203/rs.3.rs-251301/v1

Abstract

Bi_2S_3, 5 ml EG-Bi_2S_3, 10 ml EG-Bi_2S_3 was synthesized by employing solvothermal route. X-ray diffraction, UV-vis absorption, photoluminescence, Raman, scanning electron microscopic studies confirmed the structural, optical, morphological behaviors. The XRD pattern of Bi_2S_3, 5 ml EG-Bi_2S_3, 10 ml EG-Bi_2S_3 correlated well with JCPDS # 65-2435. The crystallite size was found to be 57, 49 and 40 nm. The photoluminescence spectra showed the semiconducting property of the prepared Bi_2S_3, 5 ml EG-Bi_2S_3, 10 ml EG-Bi_2S_3. The absorption spectra of the Bi_2S_3, 5 ml EG-Bi_2S_3, 10 ml EG-Bi_2S_3 nanorods were well matched with the spectra of the previous report. The band gap of the Bi_2S_3, 5 ml EG-Bi_2S_3, 10 ml EG-Bi_2S_3 was calculated to be 1.56, 1.45 and 1.3 eV in reducing order. The morphology of the Bi_2S_3, 5 ml EG-Bi_2S_3, 10 ml EG-Bi_2S_3 samples showed the development of nanorods. 10 ml EG-Bi_2S_3 sample showed better development of nanorods with the addition of ethylene glycol. The agglomeration was considerably reduced with the mixing of solvent. 10 ml EG- Bi_2S_3 sample investigated showed 86% of efficiency towards dye degradation. The narrow band gap, defined morphology of 10 ml EG- Bi_2S_3 made a positive result towards efficient photocatalytic activity.

1. Introduction

Wastewater management has become an art nowadays. By better management skills, the heavy water scarcity created in this era in all developing and developed countries will be eliminated. Wastewater is drained out in tonnes of liters. Wastewater has been increased tremendously due to the high rate of developed industries which uses dyes, organic and inorganic salts, carcinogenic substances that are fairly combined with wastewater which pulled out form industries without pre-treatment. This causes a very adverse effect on aquatic, mankind and soil's fertility. These changes surely give upon all kinds of alternates in environmental cycle (Wang et al.2020). Not only dye industries, but from other skincare product industries and pharmaceuticals, there is also toxins and chemicals that are added to the water that is flushed out of industries (Recsetar et al.2021). Even the years move on, the chemical contaminants were added in wastewater that create more hardness to the water and it critically makes the researchers to reduce the contaminants from water and changes it to reuse (Hara yamamura et al.2020). By survey scan, over large increment in textile industries has been responsible for dye molecules that are mixed with the wastewater. Dyes has the high color, strong bonding and these molecules are very hard to remove (Alderete et al.2021). There is clear classification of dyes that includes acid, basic, azoic, disperse, reactive and direct dyes. Among these azoic, sulfur dyes will not dissolve in water and these molecules are not a competent that destroys the wastewater. Other group of dyes is soluble in water. These dyes exhibit high stability and strong bonds that are not much easy one to separate from water (Hassan et al.2018). Twenty five groups of dyes were identified now. Dyes are mostly used as color aerating agents. Among different dyes, methylene blue is commonly used in most of textile industries (Wang et al.2007). Methylene blue is 3, 7 – bis dimethylamine phenothlazin 5-ium chloride compound comes under synthetic basic dye family. This methylene blue dye is cationic which is highly stable and non- biodegradable. MB is mostly used as coloring agent and in medical it was used to find the blocks in

heart and it has wide applications in medical field. However, over dosage of this dye will cause severe ailments in human beings and waste water mixed with water resources will make a adverse effects on aquatic animals (Soni et al.2020,Banerjee et al.2018).

To remove these types of organic pollutants various ways have been followed. Traditional, chemical and biological methods were followed. Traditional method has become out of fashion because these method is high cost and low efficiency. Advanced oxidation process (AOP) is the best method listed as compared with other process (Luo et al.2021). Photocatalysis is one among the AOP process which uses light sources as its basic element. The catalyst added dye solution is exposed to light illumination which excites the particles by giving photon energy and excites the particles from valence band to conduction band. The excited particles degrade the dye obtained in the solution. This process involves by creating four types of radicals like hydroxyl radicals, superoxide radicals, holes and electrons (Du et al.2021,Xu et al.2020). From all these aspects, photocatalysis is considered to be the best system for wastewater treatment. Nanoparticles are smaller in size which possess some individual properties that includes high surface to volume ratio, better optical properties and magnetic properties. These nanoparticles give good adsorption, better reaction rates and catalytic process. Hence, nanoparticles are widely used in all fields to attain the target (Singh et al.2012). The main theme of photocatalysis is that using visible light than UV light which will be considered to be better because of the negative impacts of UV light and the other reason is that, the sunlight has only 3% of the UV light spectra and most of visible light region. For practical application convenience sake, the visible light is preferred. Sulfide based materials shows good comeback because of the narrow bandgap of metal sulfide materials. This behavior is most positive one for the metal sulfides which makes it more active in photocatalytic applications and many reports were present in metal sulfides based photo degradation of methylene blue, rhodamine B and methyl orange dyes (Li et al.2012). Bismuth sulfides possess Bi_2S_3 formula is a semiconductor material with narrow bandgap of 1.4 eV. Bi_2S_3 has been reported as an excellent performance on photocatalytic dye degradation applications (Zhang et al.2003). The physico-chemical properties which directly influence the photocatalytic activity are morphology, crystal size and phase. Different synthesis methods for Bi_2S_3 have been studied and reported so far (Ghanbari et al.2014, Sakthivel et al.2020, Ye et al.2020). Various morphologies like nanorods, nanoflowers, nanodots, nanowires are developed and investigated for photo based applications (Zhang et al.2001,Xia et al.2016, Wu et al.2020, Koh et al.2003).

Kumar et.al., synthesized bismuth sulfide nanotubes by facile solvothermal process and degraded Methylene blue dye under UV- light irradiation. Ravindranath and his labmates fabricated ZnO nanosheets anchored with BiS and degraded tetracycline under solar light with 98% efficiency. Jing Huang et.al prepared different morphologies of Bi_2S_3 and investigated photocatalytic activities of the synthesized different morphologies with different dyes. Shewta Sharma, Rakshit Ameta et. al., synthesized bismuth sulfide and studied different parameters like pH, amount of semiconductor and light intensity for degrading rose Bengal dye. Wenjun Wang et.al., prepared $Bi_2O_2CO_3/Bi_2S_3$ heterojunctions and investigated photocatalytic activity. Surbhi Sharma and Nneeraj Khare developed Bi_2S_3 naoflowers by hydrothermal method and analyzed the photo degradation. Ahmed Helal et. al., synthesized Bi_2S_3

nanorods through hydrothermal method and obtained ~ 98% of efficiency on degrading MB dye for about 60 minutes irradiation time. Cathie Lee, Meei-MeiGui and their crew prepared Bi_2S_3 modified MoS_2 and investigated the efficiency. Dasari Ayodhya and Gultene Veerabhadram synthesized GO- Bi_2S_3 by sonochemical method and used to detect the flow of concentration of Hg^{2+}. Xinshan Rong et.al., prepared Bi_2S_3/ gC_3N_4 and analyzed RhB degradation (Kumar et al.2016, Koutavarapu et al.2020, Huang et al.2013, Sharma et al.2013, Helal et al.2016, Lee et al.2017, Ayodhya et al.2018, Rong et al.2015).

In this study, Bismuth Sulfide (Bi_2S_3) were prepared by employing solvothermal route by using ethylene glycol (EG) and deionised water as solvent. Bi_2S_3 nanorods were investigated by standard characterization studies. Bismuth sulfide nanorods optical properties was analyzed employing UV-vis spectroscopical studies and photoluminescence studies. The prepared nanorods morphology was studied with help of sscanning electron microscope. The development of nanorods has been thoroughly studied and its behavior towards photocatalytic dye degradation was investigated under visible light irradiation. The nanorods exhibited a good photocatalytic performance with high electron hole combination. Methylene blue dye was considerably degraded with almost 80% efficiency.

2. Materials And Methods

Bismuth nitrate ($Bi(NO_3)_3$), Thiourea, ethylene glycol, deionised water, ethanol, methanol, Whatmann filter paper were purchased form Sigma Aldrich with analytical grade. The chemicals were used without further purification. 0.01 M of Bismuth nitrate was suspended in 35 ml DI water and stirred using magnetic stirrer for complete dissolving. 0.03 M of thiourea is dissolved in 35 of DI water and stirred under magnetic stirrer. After completely dissolving, the thiourea solution is added drop wise to bismuth nitrate and completely stirred for about 1 hour to make it homogeneous. For the second solution, the same molarities ratio for $Bi(NO_3)_3$ and thiourea was taken as used before and the solvent comprised of 30 ml DI water and 5 ml ethylene glycol. Other procedure was followed as before. In the third solution, the solvent mixture ratio was changed to 25 ml DI water and 10 ml ethylene glycol and the other procedure was the same followed for the first solution. All these three solutions were autoclaved at 160^0c for 16 hours. After cooling down hydrothermal to room temperature, the black precipitate is collected and cleaned with demonized water, ethanol and methanol for about four times and it was kept in oven. The dried product is grinded and stored for further use. The structural, optical, vibrational properties were examined by X-ray diffraction studies, UV- vis absorption studies, photoluminescence studies, Raman studies. The grown nanorods morphology was studied by Scanning Electron Microscopic studies. Bi_2S_3 nanorods photocatalytic action was performed by degrading Methylene blue dye.

3. Results And Discussion

Bi_2S_3 structure was substantiated with standard JCPDS card is given in Fig. 1. The prepared pure Bi_2S_3, 5 ml EG-Bi_2S_3, 10 ml EG-Bi_2S_3 material structure was correlated with standard JCPDS. The obtained XRD pattern is in good agreement with JCPDS Card # 65-2435 with orthorhombic pattern with pbnm (62)

space group. The 2θ values with hkl values at (020), (120), (130), (310), (230), (400), (240), (041), (510), (002), (431) and (132) were resembled with the JCPDS card (Jin et al.2013). The crystalline sizes were calculated by Scherer formula used in previous literature (Kuar et al.2013). The calculated crystallite sizes of pure Bi_2S_3, 5 ml EG-Bi_2S_3, 10 ml EG-Bi_2S_3 was found to be 57 nm, 49 nm and 40 nm. The crystalline size of the samples were considerably reduced for 10 ml EG – Bi_2S_3 sample due to the addition of the solvent ethylene glycol (Kanade et al.2006). The higher angle peak shift occurred for 10 ml EG-Bi_2S_3 is due to the maximum absorption of ethylene glycol and the growth of nanorods towards the corresponding plane (Zhao et al.2016).

The photoluminescence spectra of the pure Bi_2S_3, 5 ml EG-Bi_2S_3, 10 ml EG-Bi_2S_3 sample at excitation wavelength of 420 nm was given in Fig. 2. There are three clear peaks at 470, 485 and 487 nm. These peaks clearly illustrate the semiconductor properties of the material. The peak at 485 and 487 nm is created due to the presence of some structural defects on Bi_2S_3 nanorods. The smaller nanorods with the effect of addition of ethylene glycol that are also a relevant option on the structural defect caused in the Bi_2S_3 (Kawade et al.2014).

The optical property of the pure Bi_2S_3, 5 ml EG-Bi_2S_3, 10 ml EG-Bi_2S_3 was analyzed by UV-vis absorption spectra as depicted in Fig. 3. The broad absorption at 250 nm is due to the blue shift of the Bi_2S_3 sample. The bandgap energy was found with the Tauc's plot. The bandgap values calculated were 1.56, 1.45 and 1.3 eV for pure Bi_2S_3, 5 ml EG-Bi_2S_3, 10 ml EG-Bi_2S_3. The bandgap values were decreased for 10 ml EG-Bi_2S_3 sample. The bandgap was reduced to the reported value of Bi_2S_3. The reduce in bandgap will make the sample more efficient in visible light region. Reducing the bandgap value and deciding the narrow bandgap revealed to be more active in visible light region and it can have high possibility range in making real time applications (Salavati et al.2013; Xue et al.2014).

Vibrational properties of the pure Bi_2S_3, 5 ml EG-Bi_2S_3, 10 ml EG-Bi_2S_3 samples were characterized by Raman spectra as given in Fig. 4. A clear distinct peak at 962 cm^{-1} is observed. This 962 cm^{-1} peak explored Raman bands of Bi_2S_3 nanorods. This band also confirms the sulfide band of the Bi_2S_3. This result is also in good correlation as reported (Noordeen et al.2018; Panigrahi et al.2013).

The morphology of the pure Bi_2S_3, 5 ml EG-Bi_2S_3, 10 ml EG-Bi_2S_3 was studied by Scanning Electron Microscopy. Figure 5(a-f) illustrates the development of nanorods of pure Bi_2S_3, 5 ml EG-Bi_2S_3, 10 ml EG-Bi_2S_3. Morphology of pure Bi_2S_3 was defined to be the initial stage of formation of undefined nanorods which is clearly shown in 1μm scale (Fig. 5a). In Fig. 5d, smaller nanorods of Bi_2S_3 is confirmed. Figure 5(b,e) revealed the morphology of nanosheets arranged in a clubbed manner. The agglomeration was decreased due to the addition of ethylene glycol. The thicker nanorods were started to decrease the size. The 10 ml EG-Bi_2S_3 showed a distinct growth of nanorods in a well defined manner. The addition of EG helps to grow the clear morphology of nanorods. There is a no agglomeration on the surface of nanorods. The solvent provided a better enhancement of nanorods development. The little agglomeration present on the surface of nanorods was clearly shown in Fig. 5(f) at 500 nm scale. The agglomeration

was present on the other lesser ratio samples. The morphology plays a vital role in photocatalytic activity. The larger particles will decrease the photocatalytic performance by inhibiting active photoelectron charge to in Bi_2S_3. The clear and thin nanorods will better promote the charge transfer and makes the photocatalytic activity more fast and good. The decrease in size of nanorods corroborated with XRD results. The prepared nanorods will enhance the photocatalytic activity. 10 ml EG- Bi_2S_3 sample will give an efficient output with good degradation percentage (Drmosh et al.2020; Zhu et al.2008; Miniach et al.2018).

Photocatalytic activity

The prepared pure Bi_2S_3, 5 ml EG-Bi_2S_3, 10 ml EG-Bi_2S_3 samples were further investigated for its photocatalytic activity. The sample was get ready for 50 ml. The catalyst loaded was 0.1 g. The catalyst is added into 50 ml dye and stirred in dark about 30 min. All the solutions were kept in annular type photoreactor. Then, the solution was kept without disturbing for one hour to increase the absorption equilibrium of the dye with the catalyst. The visible light with 500 W was irradiated on the samples and the liquid sample was collected for every 20 minutes.

The degradation was examined by employing UV-vis absorption spectra as depicted in Fig. 6(a-d). The absorbance peak of Methylene blue at 609 nm and 668 nm was gradually decreased which was evident from the absorbance spectra. The degradation efficiency was calculated by the formula; Degradation % = $[(A_0-A_t]/A_0)\times100]$, where A_0 is initial absorbance at 0 minutes and A_t is absorbance at t = 20, 40,… The degradation efficiency calculated was 55 %, 72 %, 73% and 86% for MB solution without catalyst, pure Bi_2S_3, 5 ml EG-Bi_2S_3 and 10 ml EG- Bi_2S_3. The efficiency was confirmed better for 10 ml EG-Bi_2S_3 sample (Kumar et al.2016).

Figure 7 shows the relative concentration of the MB dye over time. The concentration of the Methylene Blue was decreased for the 10 ml EG- Bi_2S_3 sample and correlated with UV-vis absorption spectra. When the light was passed on the solution, the electrons present in the catalyst absorbs the photon and gets excited. Valence band (VB) electrons will get sufficient energy and transfers to conduction band (CB). The excited electrons will degrade Methylene blue molecules. When samples were subjected to light irradiation for certain hours, the catalyst completely degraded the dye molecules. From these three samples 10 ml EG-Bi_2S_3 sample gives almost 86% of degradation. The morphology plays significant effect on photocatalytic process. The developed nanorods have a potential of degrading the dye molecules with complete efficiency. The undeveloped nanorods of the other two samples also showed good efficiency nevertheless the third sample with developed nanorods and less agglomeration gives higher output. Moreover, the band gap was also reduced which is more effective to work under visible light irradiation (Sharma et al.2017; Sarkar et al.2016). Addition of ethylene glycol does not directly involve in dye degradation but helps in better morphology growth. The reduce in thickness and agglomeration on nanorods efficiently attained the output which is desirable.

Figure 8 shows the bar chart of efficiency of the samples. The superior photocatalytic activity of 10 ml EG-Bi_2S_3 was optimized by adding 10 ml of ethylene glycol solvent, the uniformly developed nanorods and narrow bandgap. The main criteria for productive photocatalytic behavior are the narrow bandgap which is attained for 10 ml EG-Bi_2S_3 that produces a better results under visible light irradiation (He et al.2017).

4. Conclusion

Wastewater management is the most important issue that was going on in this era. To make use of the wastewater for some other domestic purposes without harming the users have become the toughest job to complete. Pure and ethylene glycol assisted Bi_2S_3 nanorods were synthesized by facile solvothermal route. Prepared samples explored orthorhombic structure. The crystalline size was also found and there were no extra peak identified and confirmed the purity of the prepared samples. Band gap energy of the samples was calculated to be 1.56, 1.44 and 1.3 eV. The band gap was decreased and becomes narrow which is the most positive side of 10 ml EG-Bi_2S_3. The undeveloped and developed nanorods were confirmed by SEM characterization. The growth of the nanorods was due to the addition of optimum amount of ethylene glycol. Ethylene glycol supported the growth of nanorods by reducing the agglomeration on the surface of Bi_2S_3. The nanorods provided the good photocatalytic degrading the synthetic dye under visible light for 2 hours. 86% of efficiency was obtained for 10 ml EG- Bi_2S_3. The narrow bandgap made the sample very efficient to work under visible light. The prepared nanorods are made of the uniform arrangement of the nanoparticles which absorbs light with most of its formation. 10 ml EG-Bi_2S_3 samples possess most positive behaviors of narrow bandgap and uniform nanorods which helped the sample to develop high rate of photo generated electrons and recombination of electron-hole pairs that reduced the toxic dye within short duration of time. 10 ml EG-Bi_2S_3 sample will be the most promising candidate for the future real time application on wastewater management.

Declarations

Acknowledgements

Authors would like thank Alagappa University, Karaikudi, India, for providing the research facilities to carry out this work in time.

Authors' contributions

SPK, RY, PSK, GR, DV and DVNV investigated the on the removal of toxic dye from aquatic system using nano-catalyst and the manuscript was written by them. RY and PSK analysed and interpreted the experimental results and supervised the work. All authors read and approved the final manuscript.

Data Availability

All data generated or analyzed during this study are included in this published article.

Compliance with ethical standards

Competing interests

The authors declare that they have no competing interests

Ethics approval and consent to participate: It is not applicable to this manuscript.

Consent for publication: It is not applicable to this manuscript.

Funding support: Not applicable

References

Alderete, B.L., da Silva, J., Godoi, R., da Silva, F.R., Taffarel, S.R., da Silva, L.P., Garcia, A.L.H., Júnior, H.M., de Amorim, H.L.N. and Picada, J.N., 2021. Evaluation of toxicity and mutagenicity of a synthetic effluent containing azo dye after advanced oxidation process treatment. *Chemosphere*, *263*, p.128291.

Ayodhya, D. and Veerabhadram, G., 2018. Highly efficient sunlight-driven photocatalytic degradation of organic pollutants and fluorescence detection of Hg2+ using multifunctional GO-Bi2S3 nanostructures. *Journal of Photochemistry and Photobiology A: Chemistry*, *356*, pp.545-555.

Banerjee, S., Benjwal, P., Singh, M. and Kar, K.K., 2018. Graphene oxide (rGO)-metal oxide (TiO2/Fe3O4) based nanocomposites for the removal of methylene blue. *Applied surface science*, *439*, pp.560-568.

Drmosh, Q.A., Hezam, A., Hendi, A.H.Y., Qamar, M., Yamani, Z.H. and Byrappa, K., 2020. Ternary Bi2S3/MoS2/TiO2 with double Z-scheme configuration as high performance photocatalyst. *Applied Surface Science*, *499*, p.143938.

Du, C., Zhang, Z., Yu, G., Wu, H., Chen, H., Zhou, L., Zhang, Y., Su, Y., Tan, S., Yang, L. and Song, J., 2021. A review of metal organic framework (MOFs)-based materials for antibiotics removal via adsorption and photocatalysis. *Chemosphere*, p.129501.

Ghanbari, D., Salavati-Niasari, M., Karimzadeh, S. and Gholamrezaei, S., 2014. Hydrothermal synthesis of Bi_2S_3 nanostructures and ABS-based polymeric nanocomposite. *Journal of Nanostructures*, *4*(2), pp.227-232.

Hara-Yamamura, H., Fukushima, T., Tan, L.C. and Okabe, S., 2020. Transcriptomic analysis of HepG2 cells exposed to fractionated wastewater effluents suggested humic substances as potential inducer of whole effluent toxicity. *Chemosphere*, *240*, p.124894.

Hassan, M.M. and Carr, C.M., 2018. A critical review on recent advancements of the removal of reactive dyes from dyehouse effluent by ion-exchange adsorbents. *Chemosphere*, *209*, pp.201-219.

He, H.Y., 2017. Facile synthesis of Bi2S3 nanocrystalline-modified TiO2: Fe nanotubes hybrids and their photocatalytic activities in dye degradation. *Particulate Science and Technology*, *35*(4), pp.410-417.

Helal, A., Harraz, F.A., Ismail, A.A., Sami, T.M. and Ibrahim, I.A., 2016. Controlled synthesis of bismuth sulfide nanorods by hydrothermal method and their photocatalytic activity. *Materials & Design*, *102*, pp.202-212.

Huang, J., Zhang, H., Zhou, X. and Zhong, X., 2013. Dimensionality-dependent performance of nanostructured bismuth sulfide in photodegradation of organic dyes. *Materials Chemistry and Physics*, *138*(2-3), pp.755-761.

Jin, R., Liu, J., Li, G. and Yang, L., 2013. Solvothermal synthesis and good electrochemical property of pinetree like Bi2S3. *Crystal Research and Technology*, *48*(12), pp.1050-1054.

Kanade, K.G., Kale, B.B., Aiyer, R.C. and Das, B.K., 2006. Effect of solvents on the synthesis of nano-size zinc oxide and its properties. *Materials Research Bulletin*, *41*(3), pp.590-600.

Kawade, U.V., Panmand, R.P., Sethi, Y.A., Kulkarni, M.V., Apte, S.K., Naik, S.D. and Kale, B.B., 2014. Environmentally benign enhanced hydrogen production via lethal H 2 S under natural sunlight using hierarchical nanostructured bismuth sulfide. *RSC Advances*, *4*(90), pp.49295-49302.

Koutavarapu, R., Reddy, C.V., Syed, K., Reddy, K.R., Shetti, N.P., Aminabhavi, T.M. and Shim, J., 2020. Ultra-small zinc oxide nanosheets anchored onto sodium bismuth sulfide nanoribbons as solar-driven photocatalysts for removal of toxic pollutants and phtotoelectrocatalytic water oxidation. *Chemosphere*, p.128559.

Koh, Y.W., Lai, C.S., Du, A.Y., Tiekink, E.R. and Loh, K.P., 2003. Growth of bismuth sulfide nanowire using bismuth trisxanthate single source precursors. *Chemistry of materials*, *15*(24), pp.4544-4554.

Kumar, S., Sharma, S., Umar, A. and Kansal, S.K., 2016. Bismuth sulphide (Bi2S3) nanotubes as an efficient photocatalyst for methylene blue dye degradation. *Nanoscience and Nanotechnology Letters*, *8*(3), pp.266-272.

Kumar, S.S., Venkateswarlu, P., Rao, V.R. and Rao, G.N., 2013. Synthesis, characterization and optical properties of zinc oxide nanoparticles. *International Nano Letters*, *3*(1), pp.1-6.

Li, X., Zhu, J. and Li, H., 2012. Comparative study on the mechanism in photocatalytic degradation of different-type organic dyes on SnS2 and CdS. *Applied Catalysis B: Environmental*, *123*, pp.174-181.

Lee, W.C., Gui, M.M., Tan, L.L., Wu, T.Y., Sumathi, S. and Chai, S.P., 2017. Bismuth sulphide-modified molybdenum disulphide as an efficient photocatalyst for hydrogen production under simulated solar

light. *Catalysis Communications*, *98*, pp.66-70.

Luo, H., Zhou, X., Guo, X., Fang, Z., Chen, Q. and Zhou, J., 2021. WS2 as highly active co-catalyst for the regeneration of Fe (II) in the advanced oxidation processes. *Chemosphere*, *262*, p.128067.

Miniach, E. and Gryglewicz, G., 2018. Solvent-controlled morphology of bismuth sulfide for supercapacitor applications. *Journal of Materials Science*, *53*(24), pp.16511-16523.

Noordeen, A.K., Sambasivam, S., Chinnasamy, S., Ramasamy, J. and Subramani, T., 2018. Hierarchical flower structured Bi 2 S 3/reduced graphene oxide nanocomposite for high electrochemical performance. *Journal of Inorganic and Organometallic Polymers and Materials*, *28*(1), pp.73-83.

Panigrahi, P.K. and Pathak, A., 2013. The growth of bismuth sulfide nanorods from spherical-shaped amorphous precursor particles under hydrothermal condition. *Journal of Nanoparticles*, *2013*.

Recsetar, M.S., Fitzsimmons, K.M., Cuello, J.L., Hoppe-Jones, C. and Snyder, S.A., 2021. Evaluation of a recirculating hydroponic bed bioreactor for removal of contaminants of emerging concern from tertiary-treated wastewater effluent. *Chemosphere*, *262*, p.128121.

Rong, X., Qiu, F., Yan, J., Zhao, H., Zhu, X. and Yang, D., 2015. Coupling with a narrow-band-gap semiconductor for enhancement of visible-light photocatalytic activity: preparation of Bi 2 S 3/gC 3 N 4 and application for degradation of RhB. *RSC Advances*, *5*(32), pp.24944-24952.

Sakthivel, R., Kubendhiran, S. and Chen, S.M., 2020. One-pot sonochemical synthesis of marigold flower-like structured ruthenium doped bismuth sulfide for the highly sensitive detection of antipsychotic drug thioridazine in the human serum sample. *Journal of the Taiwan Institute of Chemical Engineers*, *111*, pp.270-282.

Salavati-Niasari, M., Behfard, Z., Amiri, O., Khosravifard, E. and Hosseinpour-Mashkani, S.M., 2013. Hydrothermal synthesis of bismuth sulfide (Bi 2 S 3) nanorods: Bismuth (III) monosalicylate precursor in the presence of thioglycolic acid. *Journal of Cluster Science*, *24*(1), pp.349-363.

Sarkar, A., Ghosh, A.B., Saha, N., Srivastava, D.N., Paul, P. and Adhikary, B., 2016. Enhanced photocatalytic performance of morphologically tuned Bi2S3 NPs in the degradation of organic pollutants under visible light irradiation. *Journal of colloid and interface science*, *483*, pp.49-59.

Sharma, S., Ameta, R., Malkani, R.K. and Ameta, S.C., 2011. Use of semi-conducting bismuth sulfide as a photocatalyst for degradation of Rose Bengal. *Macedonian Journal of Chemistry and Chemical Engineering*, *30*(2), pp.229-234.

Sharma, S. and Khare, N., 2018. Hierarchical Bi2S3 nanoflowers: A novel photocatalyst for enhanced photocatalytic degradation of binary mixture of Rhodamine B and Methylene blue dyes and degradation of mixture of p-nitrophenol and p-chlorophenol. *Advanced Powder Technology*, *29*(12), pp.3336-3347.

Sharma, S. and Khare, N., 2017, May. Synthesis of bismuth sulfide nanostructures for photodegradation of organic dye. In *AIP Conference Proceedings* (Vol. 1832, No. 1, p. 050064). AIP Publishing LLC.

Singh, S., Kumar, V., Romero, R., Sharma, K. and Singh, J., 2019. Applications of nanoparticles in wastewater treatment. In *Nanobiotechnology in bioformulations* (pp. 395-418). Springer, Cham.

Soni, S., Bajpai, P.K., Mittal, J. and Arora, C., 2020. Utilisation of cobalt doped Iron based MOF for enhanced removal and recovery of methylene blue dye from waste water. *Journal of Molecular Liquids*, *314*, p.113642.

Wang, Y., Yang, H., Sun, X., Zhang, H. and Xian, T., 2020. Preparation and photocatalytic application of ternary n-BaTiO3/Ag/p-AgBr heterostructured photocatalysts for dye degradation. *Materials Research Bulletin*, *124*, p.110754.

Wang, H., Xie, C., Zhang, W., Cai, S., Yang, Z. and Gui, Y., 2007. Comparison of dye degradation efficiency using ZnO powders with various size scales. *Journal of Hazardous materials*, *141*(3), pp.645-652.

Wang, W., Cheng, H., Huang, B., Lin, X., Qin, X., Zhang, X. and Dai, Y., 2013. Synthesis of Bi2O2CO3/Bi2S3 hierarchical microspheres with heterojunctions and their enhanced visible light-driven photocatalytic degradation of dye pollutants. *Journal of colloid and interface science*, *402*, pp.34-39.

Wu, Y., Liang, Y., Liu, Y., Hao, Y., Tao, N., Li, J., Sun, X., Liu, Y.N. and Zhou, M., Bismuth Sulfide Nanodots Embedded Hydrogel as Theranostic Platform for CT Imaging and Photothermal/Antiangiogenic Therapy. *Antiangiogenic Therapy*.

Xiao, Z., Xu, C., Jiang, X., Zhang, W., Peng, Y., Zou, R., Huang, X., Liu, Q., Qin, Z. and Hu, J., 2016. Hydrophilic bismuth sulfur nanoflower superstructures with an improved photothermal efficiency for ablation of cancer cells. *Nano Research*, *9*(7), pp.1934-1947.

Xu, B., Ahmed, M.B., Zhou, J.L. and Altaee, A., 2020. Visible and UV photocatalysis of aqueous perfluorooctanoic acid by TiO2 and peroxymonosulfate: Process kinetics and mechanistic insights. *Chemosphere*, *243*, p.125366.

Xue, B., Sun, T., Mao, F. and Xie, J., 2014. Gelatin-assisted green synthesis of bismuth sulfide nanorods under microwave irradiation. *Materials Letters*, *122*, pp.106-109.

Ye, M., Shi, F., Shen, M., Qin, W., Ren, C. and Yang, Z., 2020. Composite soft-template method synthesis and biosensing application of hedgehog-like bismuth sulfide micro-nanostructures. *Colloids and Surfaces A: Physicochemical and Engineering Aspects*, p.126094.

Zhang, H., Ji, Y., Ma, X., Xu, J. and Yang, D., 2003. Long Bi2S3 nanowires prepared by a simple hydrothermal method. *Nanotechnology*, *14*(9), p.974.

Zhang, W., Yang, Z., Huang, X., Zhang, S., Yu, W., Qian, Y., Jia, Y., Zhou, G. and Chen, L., 2001. Low temperature growth of bismuth sulfide nanorods by a hydrothermal method. *Solid state communications*, *119*(3), pp.143-146.

Zhao, W., Wu, Y., Xu, J. and Gao, C., 2016. Retraction: Effect of ethylene glycol on hydrothermal formation of calcium sulfate hemihydrate whiskers with high aspect ratios. *RSC Advances*, *6*(102), pp.99639-99639.

Zhu, G., Liu, P., Zhou, J., Bian, X., Wang, X., Li, J. and Chen, B., 2008. Effect of mixed solvent on the morphologies of nanostructured Bi2S3 prepared by solvothermal synthesis. *Materials Letters*, *62*(15), pp.2335-2338

Figures

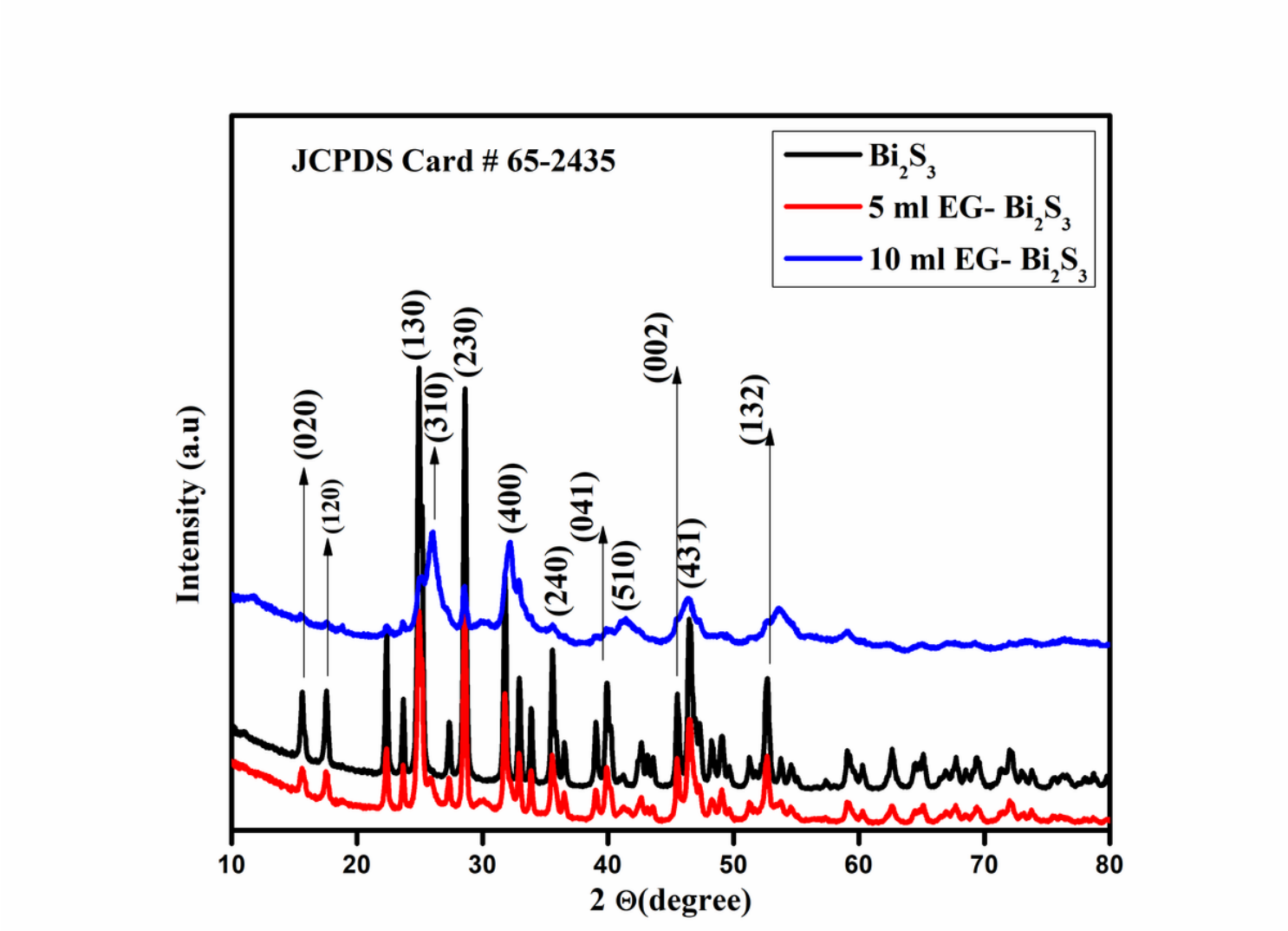

Figure 1

XRD pattern of pure Bi2S3, 5 ml EG-Bi2S3¬, 10 ml EG-Bi2S3

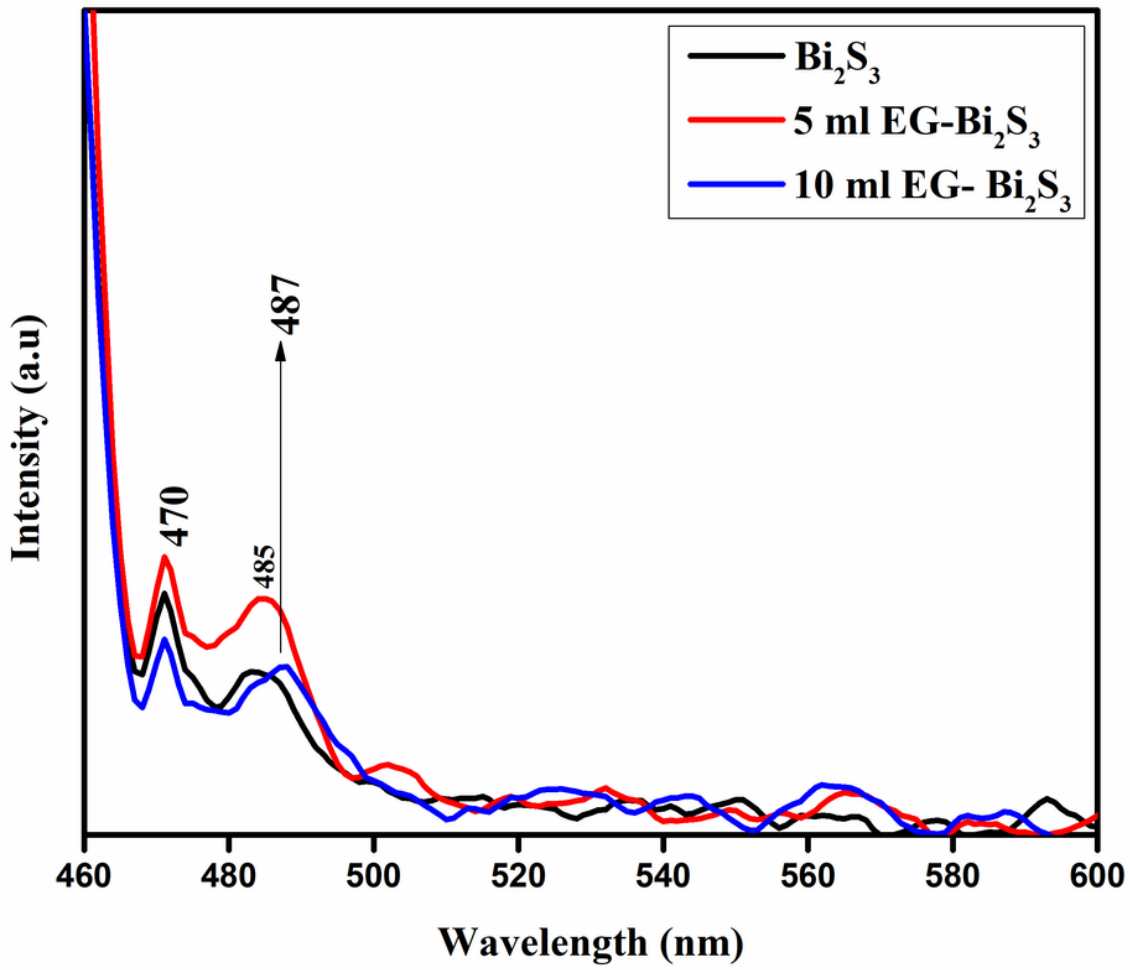

Figure 2

PL spectra of pure Bi2S3, 5 ml EG-Bi2S3¬, 10 ml EG-Bi2S3

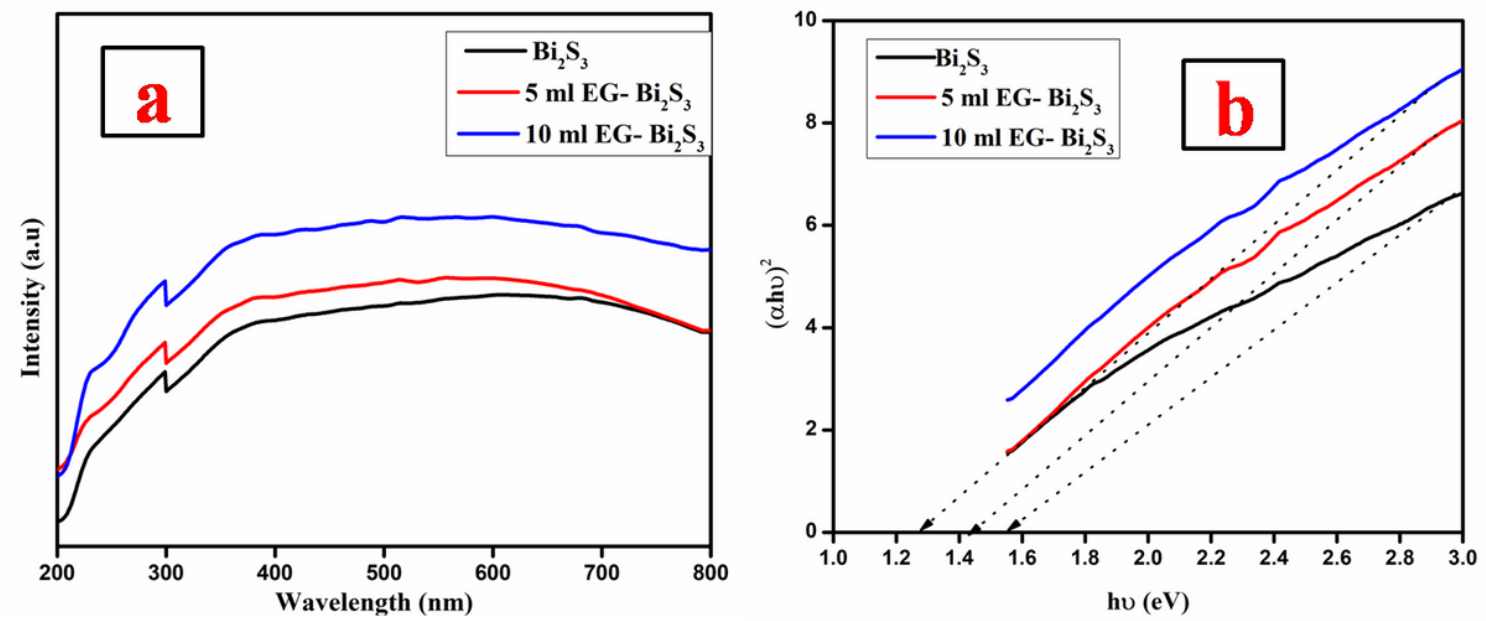

Figure 3

(a) UV- vis (b) Tauc's plot of pure Bi2S3, 5 ml EG-Bi2S3¬, 10 ml EG-Bi2S3

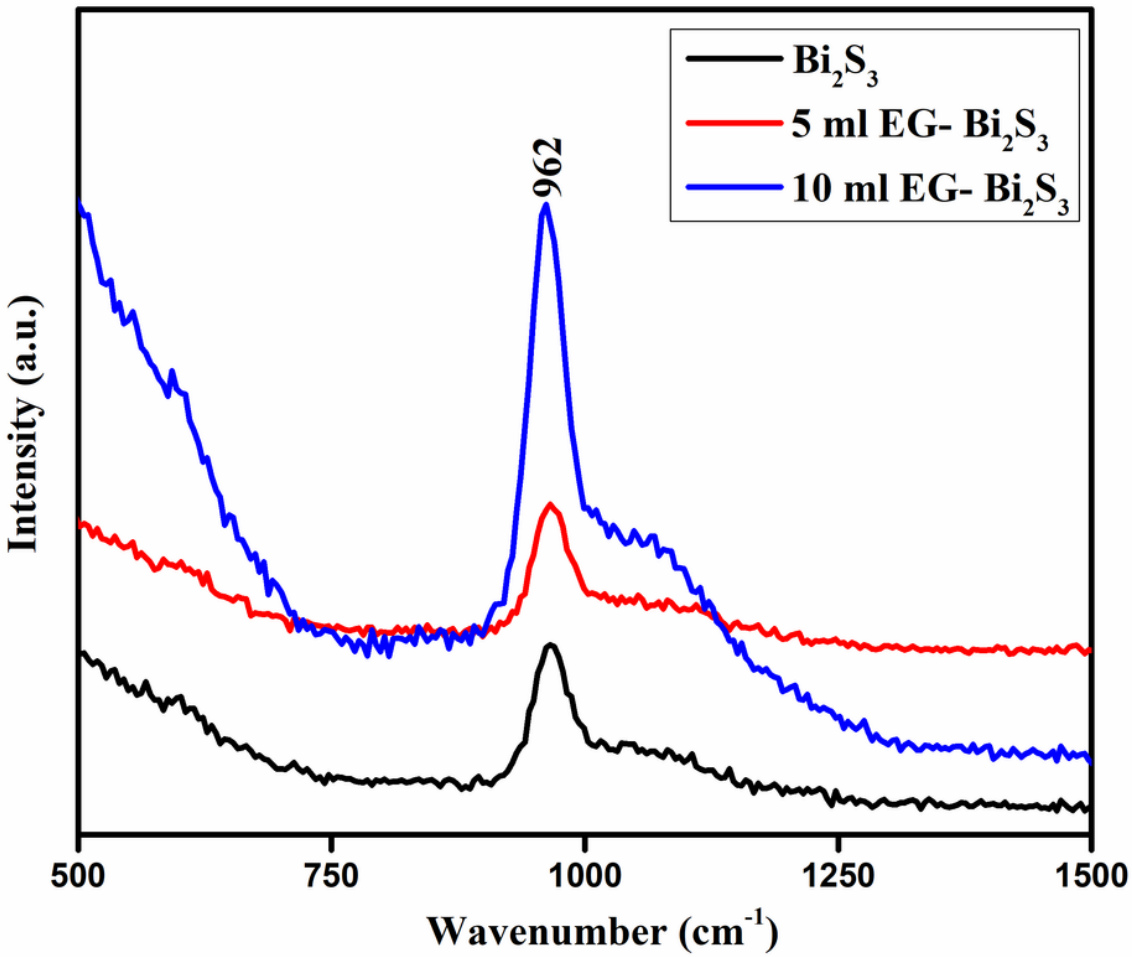

Figure 4

Raman spectra of pure Bi2S3, 5 ml EG-Bi2S3¬, 10 ml EG-Bi2S3

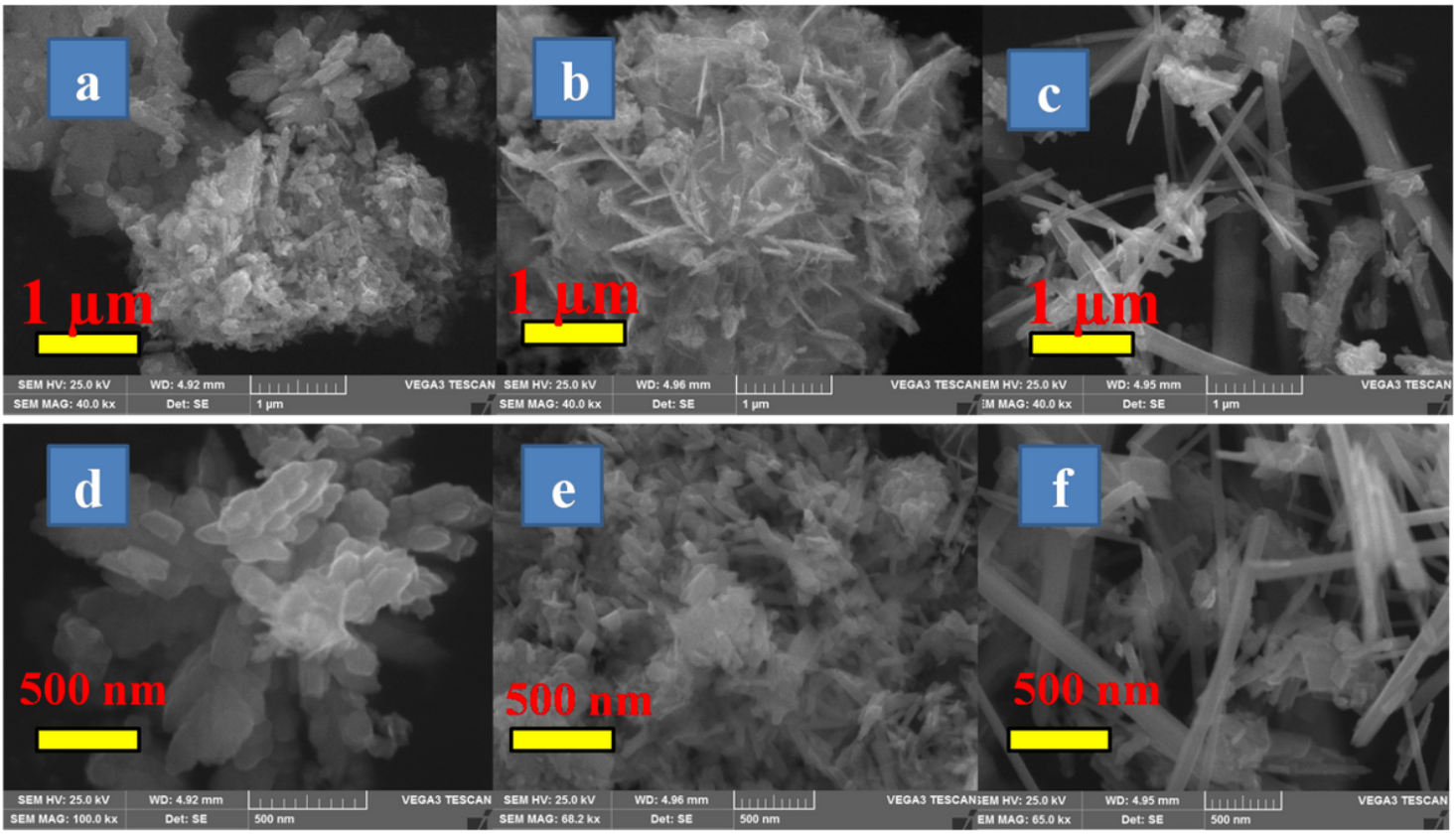

Figure 5

(a) Pure Bi2S3 at 1µm (b) 5 ml EG-Bi2S3 Bi2S3 at 1µm (c) 10 ml EG- Bi2S3 at 1µm (d) Bi2S3 at 500 nm (e) 5 ml EG- Bi2S3 at 500 nm (f) 10 ml EG- Bi2S3 at 500 nm

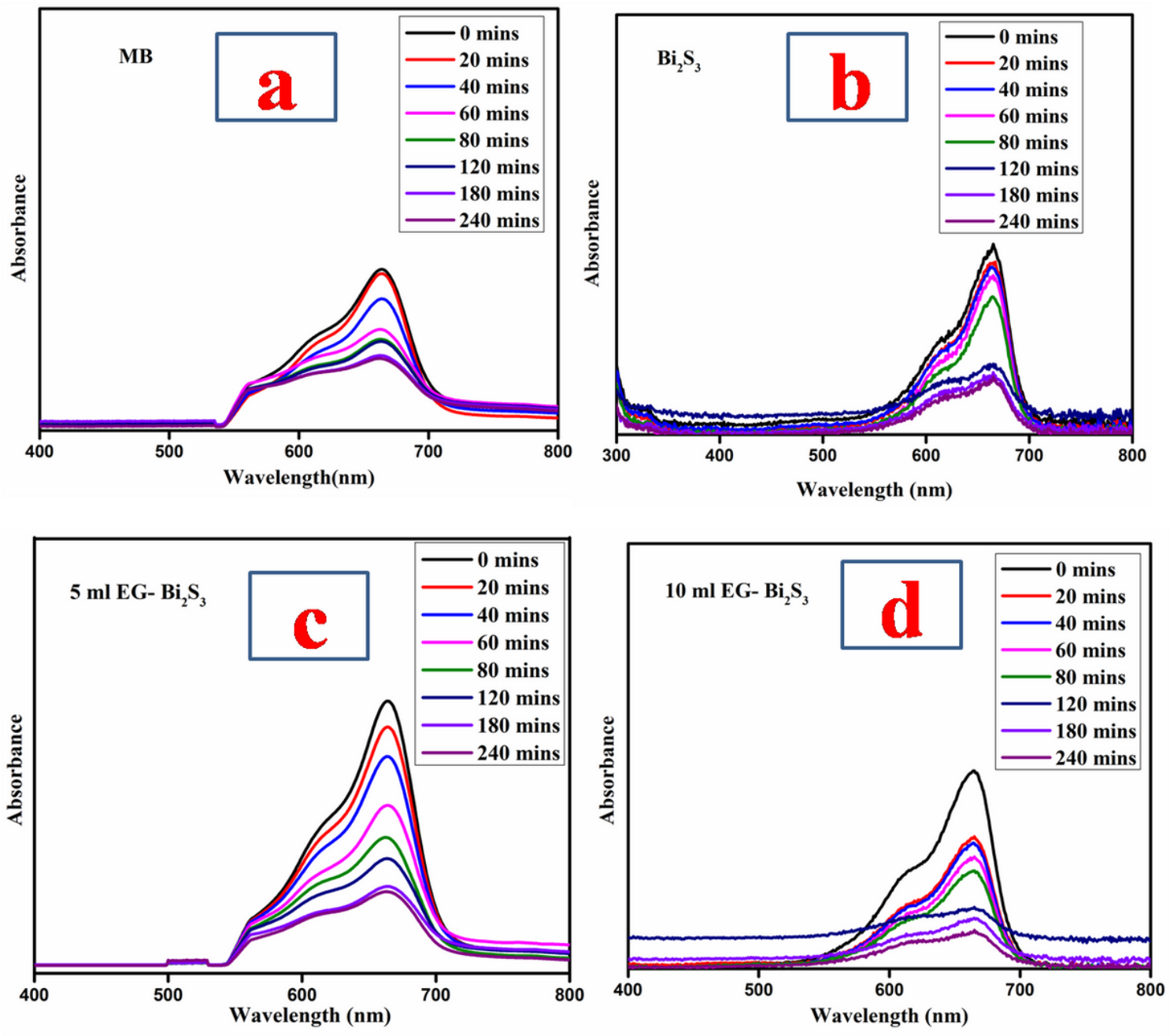

Figure 6

Absorption spectra of (a) MB dye (b) Bi2S3 loaded solution (c) 5 ml EG- Bi2S3 loaded solution (d) 10 ml EG- Bi2S3 loaded solution

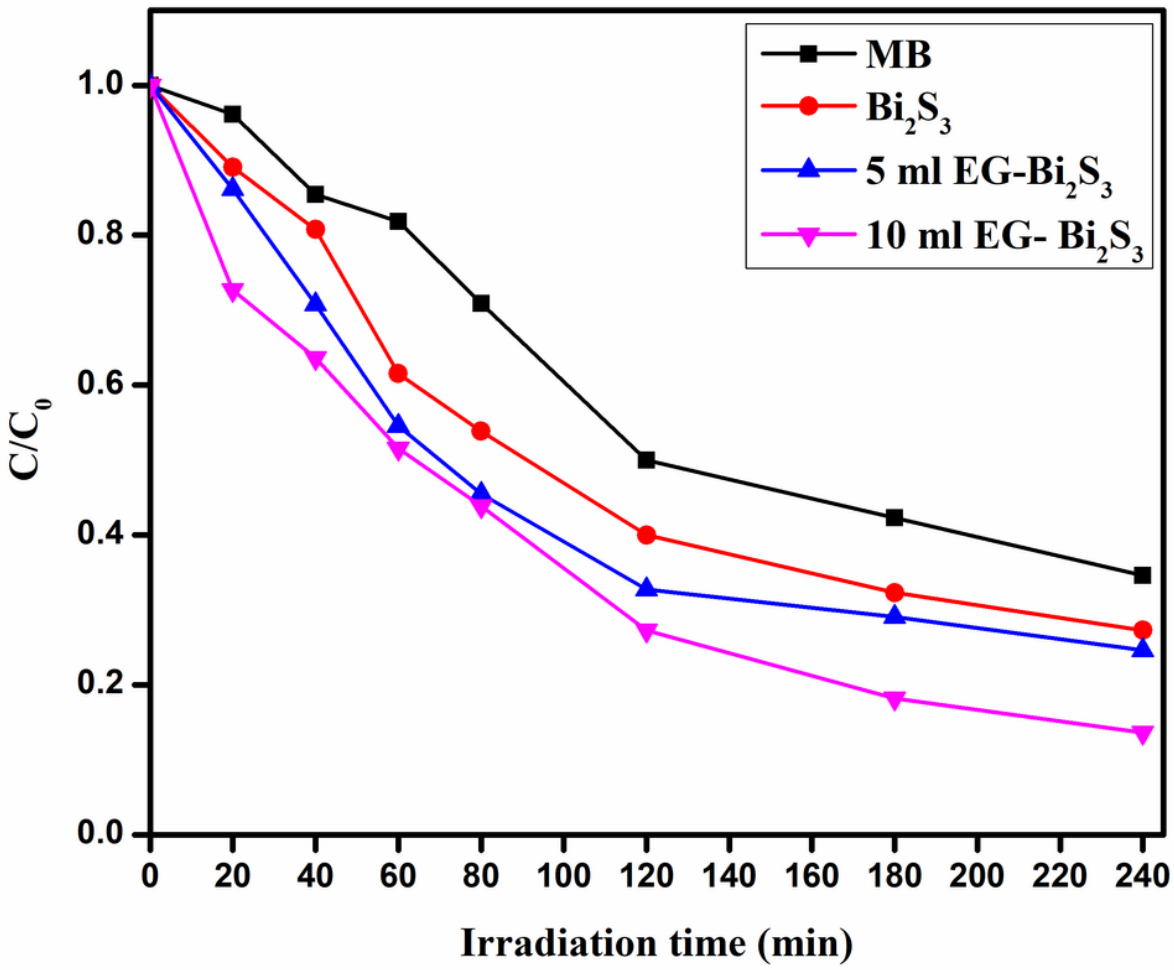

Figure 7

Relative concentration Vs. time plot of pure MB, Bi2S3, 5 ml EG- Bi2S3, 10 ml EG- Bi2S3

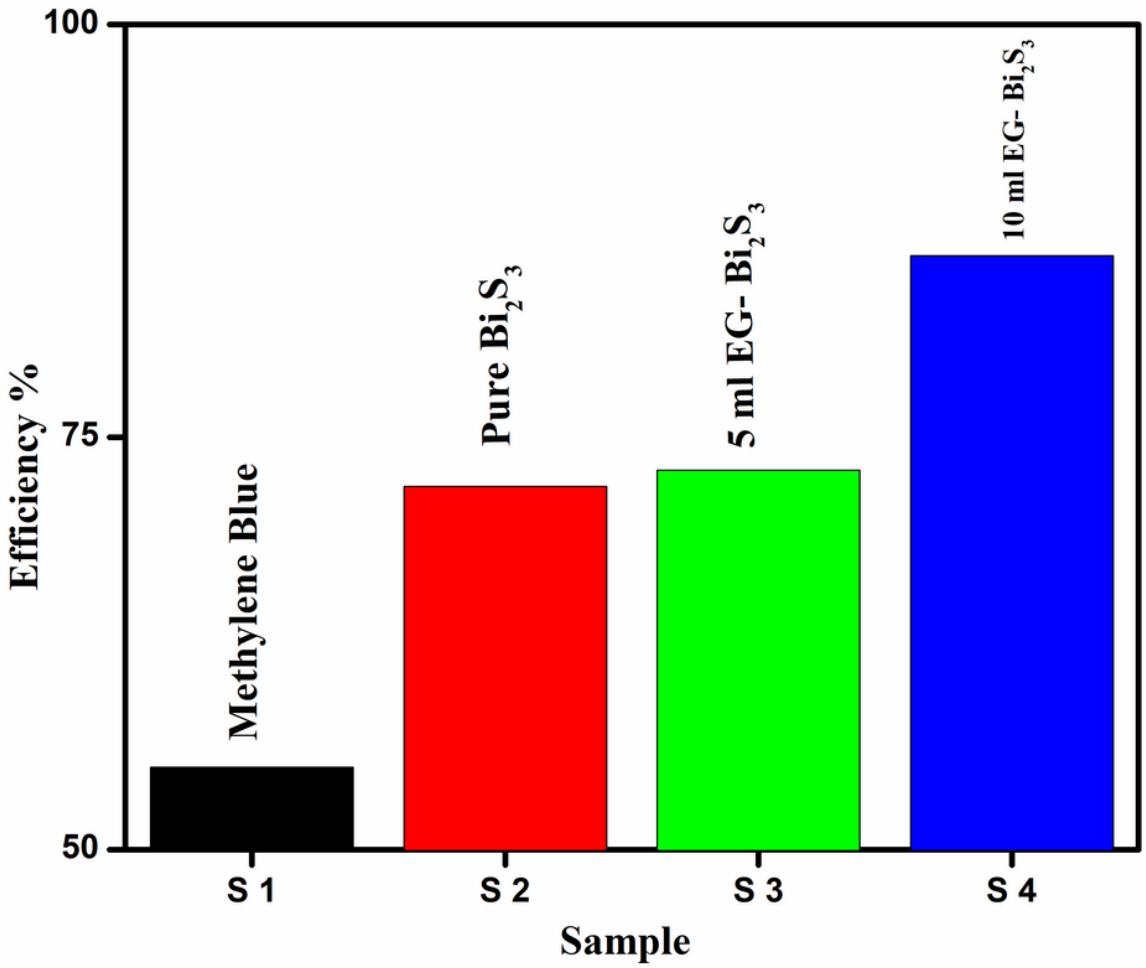

Figure 8

Efficiency plot of the pure MB, Bi2S3, 5 ml EG-Bi2S3, 10 ml EG-Bi2S3¬.